Proceedings of the Sixth International Conference on
Railway Technology: Research, Development and Maintenance
Edited by: J. Pombo
Civil-Comp Conferences, Volume 7, Paper 17.5
Civil-Comp Press, Edinburgh, United Kingdom, 2024
ISSN: 2753-3239, doi: 10.4203/ccc.7.17.5

Performance of a Ballastless Track in a Transition Zone and the Influence of the Train Speed

A. Ramos[1], A. Gomes Correia[2] and R. Calçada[1]

[1]CONSTRUCT-LESE, Faculty of Engineering, University of Porto, Porto, Portugal
[2]ISISE, School of Engineering, University of Minho Guimarães, Portugal

Abstract

The ballastless track is the most popular railway system nowadays. This is due to the associated reduced maintenance costs and operations. However, their performance in transition zones is a major concern of the Railway Infrastructure Managers. These areas are characterized by an abrupt change in the track stiffness, which leads to the development of differential settlements. Thus, it is crucial to have a methodology able to accurately predict the performance of the ballastless tracks in transition zones, mostly in the scope of high-speed lines. This work presents a detailed analysis regarding the evaluation of the performance of a ballastless track in an embankment-tunnel transition zone considering the influence of the train speed. In this analysis six different train speeds were adopted: 220 km/h, 360 km/h, 500 km/h, and 600 km/h. Moreover, the influence of the critical speed is also evaluated. The adopted and developed methodology is a novel and hybrid approach that allows including short-term and long-term performance, through the development of a powerful 3D model combined with the implementation of a calibrated empirical permanent deformation model.

Keywords: ballastless track, transition zone, train speed, high-speed lines, permanent deformation, cyclic loading.

1 Introduction

The transition zones exhibit an abrupt change in track stiffness, leading to the emergence of differential settlements and the growth of dips and bumps [1, 2].

Consequently, these transition zones stand as primary sources of issues within the railway network. Notably, the occurrence of differential settlements implies a superior number of maintenance operations, leading to substantial costs [3-5].

The problems encountered in the transition zones start with the difference in the support stiffness, resulting in differential settlements, increasing the dynamic wheel load, and amplifying the vertical train-track interaction. These problems contribute to noise generation, vibration, poor ride comfort, high risk of derailment, hanging sleepers, permanent rail deformation, ballast penetration into the subgrade, and cracking of the concrete sleepers or concrete slab[6] [7, 8].

Transition zones may have different causes: track change between a ballasted track to a ballastless track, embankment to a tunnel or bridge, and presence of a hydraulic underpass or box culvert. Nowadays, in the scope of high-speed lines, the ballastless tracks have gained popularity due to their reduced maintenance operations and costs, despite the high initial investment [9]. Despite the expected good performance of the ballastless track (even in transition zones), it is crucial to comply with the reduced deformation allowable limits, particularly concerning long-term deformations. This analysis requires advanced numerical modelling to accurately predict permanent settlements.

This work presents an assessment of the short and long-term performance of a ballastless track within a transition zone considering the influence of the train speed (including the critical speed). The acceleration of geomaterials degradation with the train speed, results in excessive settlement [10], which is a particularly challenging issue within transition zones. In this case, a transition between an embankment and a tunnel is studied in detail. This modelling includes the vehicle-track and super-substructure interactions. A hybrid approach was used to assess the track performance at various train speeds, which also include the critical speed: 220 km/h, 360 km/h, 500 km/ and 600 km/h. Short-term performance is analysed through a powerful 3D FEM model developed in ANSYS, while the permanent deformation is evaluated through the implementation of a calibrated empirical permanent deformation model designed to simulate track degradation.

2 Numerical model and methodologies

The numerical model represents a ballastless track consisting of rails, railpads, a concrete slab, HBL (hydraulically bonded layer), and a substructure that encompasses the FPL (frost protection layer) and subgrade, as depicted in Figure 1. The concrete slab presents a thickness of 0.2 m, HBL has a thickness of 0.3 m and the FPL is 0.4 m. The thickness of the subgrade is 10.5 m. The material characteristics can be found in Ramos, Gomes Correia [2], with the key properties listed in Table 1, based on prior calibration work developed by the same authors [11].

In this analysis, damping coefficients were determined using the *Rayleigh* damping matrix. Additional details are available in Ramos, Gomes Correia [2]. A frequency range of 5 Hz to 200 Hz was adopted, which is sufficient for an accurate track response.

The numerical model, as illustrated in Figure 1, spans a total length of 53.1 meters, encompassing both the 31.65-meter embankment and the 21.25-meter tunnel. To enhance computational efficiency, the symmetric boundary conditions were employed. The distance between the symmetry plane and the vertical boundary measures 6 meters, with x = 0 meters marking the transition point between the embankment and the tunnel.

The analysis is focused on the passage of the Portuguese *Alfa Pendular* train at varying speeds, including 220 km/h, 360 km/h, 500 km/h, and 600 km/h. Detailed train and model properties can be found in adapted from Ramos, Gomes Correia [2]).. In this study, the train's components include the bogies, primary suspension, mass, and wheelset axles, while incorporating Hertzian stiffness to replicate the vehicle-track interaction.

Concerning the applied load, a constant value of 67.5 kN (135/2) was adopted. To simulate both short-term and long-term track responses, the passage of the initial four bogies was simulated. To avoid spurious reflections and attenuate the waves that impinge the vertical boundaries, viscous dampers were adopted and placed in the FPL and subgrade materials using the *Lysmer* formulation.

Regarding the modelling, the materials were modelled with solid elements with 8 nodes using linear elastic models. Moreover, contact elements were implemented between the train and track to simulate the interaction between the two bodies and between the HBL and FPL to simulate the “detachment” between both elements. The dynamic analysis was performed in the software *ANSYS* using the *Newmark-Raphson* method with a time step equal to 0.002 s.

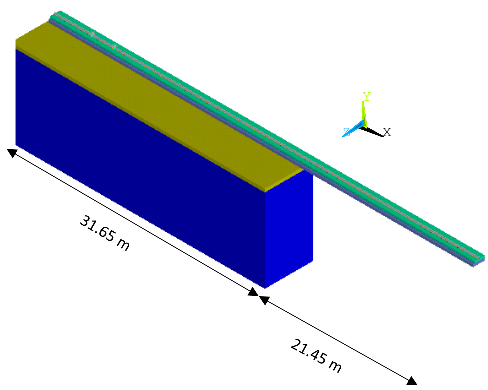

Figure 1. Numerical model.

Material	Properties		
Rail (BS113A)	E=200 ×10^9 Pa	γ=7850 kg/m^3	ν=0.3
Railpad	K=1800×10^6 N/m E=k× thickness /area	γ=1000 kg/m^3	ν=0.3
Steel plate	E=210×10^9 Pa	γ=7850 kg/m^3	ν=0.3
EPDM (ethylene propylene diene monomer)	K=40×10^6 N/m E=k× thickness /area	γ=1200 kg/m^3	ν=0.0
Cement grout	E=25×10^9 Pa	γ=2000 kg/m^3	ν=0.25
Concrete slab	E=40×10^9 Pa	γ=2500 kg/m^3	ν=0.25
HBL	E=15×10^9 Pa	γ=2400 kg/m^3	ν=0.25
FPL	E=445.5×10^6 Pa	γ=2141 kg/m^3	ν=0.35
Subgrade	E=214.5×10^6 Pa	γ=2091 kg/m3	ν=0.35

Table 1 Properties of the materials (adapted from Ramos, Gomes Correia [2]).

3 Results

The objective of this study is to examine the impact of train speed on the dynamic response of a ballastless track within a transition zone. Consequently, different simulations considering four distinct train speeds were conducted: 220 km/h, 360 km/h, 500 km/h, and 600 km/h. This wide range of speeds was selected to assess the performance of a high-speed railway line within a transition zone. Specifically, the highest speed, 600 km/h, was chosen to investigate the influence of the critical speed on the rail track's behavior, since substantial amplifications of the track's response are expected.

Short-term performance

The short-term performance assessment encompasses the analysis of displacements and accelerations induced in different track components Thus, the maximum displacements in the top of the rail and concrete slab were obtained in the alignment under the load (Figure 2). The results indicate an increase in the displacements with higher train speeds. Specifically, regarding rail displacements, a train speed of 600 km/h leads to a significant amplification in both magnitude and variation of displacements. In the concrete slab, the displacements are also scaled proportionally with the train speed, mostly in the sections far from the transition.

In addition to the displacement analysis, the vertical accelerations at the top of the concrete slab and HBL were obtained. These elements have a crucial role since allow maintaining track continuity. The results present the maximum and minimum vertical acceleration values along the track under the loading alignment. The results indicate a significant increase in accelerations corresponding to higher train speeds. However, this increase is especially pronounced in the concrete slab and HBL, particularly prior to the transition zone (x=0 m) when the train is traveling at 600 km/h. In this scenario, the acceleration surpasses the acceptable thresholds, typically set below 10 m/s^2. At the remaining speeds, the results fall within acceptable ranges. As expected, the results also illustrate a decline in vertical acceleration along the transition zone.

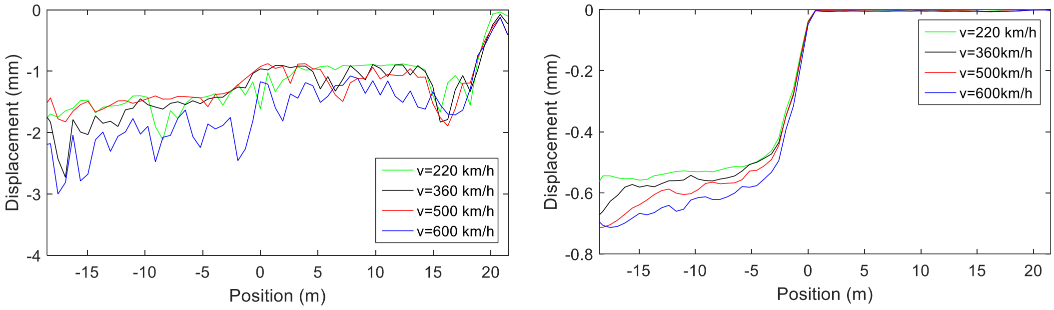

a) b)

Figure 2. Maximum displacements induced in the top of the: a) rail; b) concrete slab.

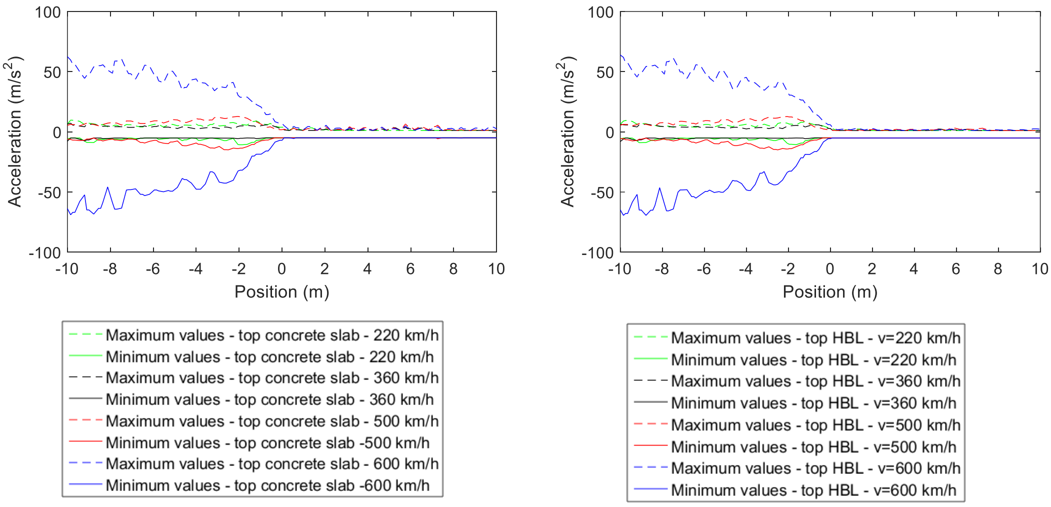

a) b)

Figure 3. Vertical accelerations on concrete slab (a) and HBL (b).

Long term performance

In this analysis, the prediction of the permanent deformation is only carried out on the FPL and subgrade, which are the geomaterials. The permanent deformation is determined by applying the empirical model developed by Chen, Chen [12]:

$$\varepsilon_1^p(N) = \varepsilon_1^{p0}\left[1 - e^{-BN}\right]\left(\frac{\sqrt{{p_{am}}^2 + {q_{am}}^2}}{p_a}\right)^a \cdot \frac{1}{m\left(1+\frac{p_{ini}}{p_{am}}\right)+\frac{s}{p_{am}}-\frac{(q_{ini}+q_{am})}{p_{am}}} \qquad (1)$$

where the parameters ε_1^{p0}, B and a are the material's constants of the model, m and s are defined by the yielding criterion $q=s+m{\cdot}p$, N is the number of loading cycles, p_{ini} and q_{ini} are the initial stress state and p_{am} and q_{am} are the stress levels induced in the subgrade during the passage of the train.

The constants employed to characterize the empirical permanent deformation model were obtained in a prior study conducted by Ramos, Gomes Correia [11]. In this context, each cycle (*N*) corresponds to the passage of one of the 24 axles of the *Alfa Pendular* train.

This methodology involves the development of a powerful 3D numerical model of the vehicle-track system within ANSYS software. From the numerical results, the stress in the subgrade and FPL are obtained in all directions and in all elements and nodes. These stress values are then exported to MATLAB to predict the permanent deformation based on the implementation of the selected empirical permanent deformation model. In this analysis, each curve of the permanent deformation corresponds to 1 million load cycles.

Despite the importance of the permanent deformation, the results are analysed in terms of cumulative permanent settlements to have the magnitude of the track's settlement:

$$\delta = \sum_{i=1}^{n} \varepsilon_{p;i} H_{s;i} \tag{2}$$

where *i* corresponds to the number of elements that constitute a certain material, $H_{s;i}$ corresponds to the thickness of each element (in m), $\varepsilon_{p;i}$ is the permanent deformation at the center of each element, and δ is the cumulative permanent deformation (in m).

Following the developed methodology, the maximum cumulative permanent settlements occurring in the FPL and subgrade were calculated under the load alignment.

As depicted in Figure 4, the results for the subgrade and FPL reveal a clear pattern: as the train speed increases, there is a corresponding increment in permanent settlements. Notably, the permanent settlements are more pronounced when the train's speed is set at 360 km/h compared to 500 km/h. However, the disparities between these two train speeds are relatively modest. The most significant increase in permanent settlements occurs when the train speed approaches the critical speed.

In the case of the FPL, the results remain below the allowable deformation threshold for slab tracks in high-speed lines, which are typically set at 30 mm. However, in the case of the subgrade, the settlement exceeds the 30 mm limit, which can be a problem. Furthermore, it is worth noting that settlements in the subgrade are more pronounced than in the FPL. Although the magnitude of the stresses is greater at the FPL, the strength properties of the track influence the development of permanent deformation such as the cohesion and friction angle. In subgrade elements, the stress paths closely approach the yielding criterion, leading to more significant settlements.

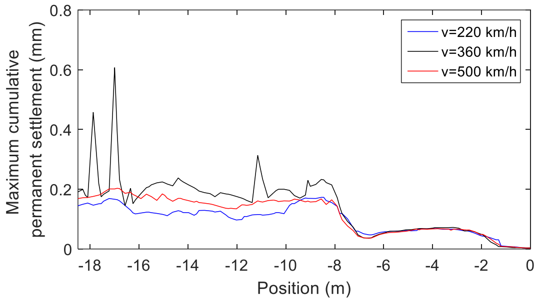

a) FPL with the train speed between 220 km/h and 500 km/h

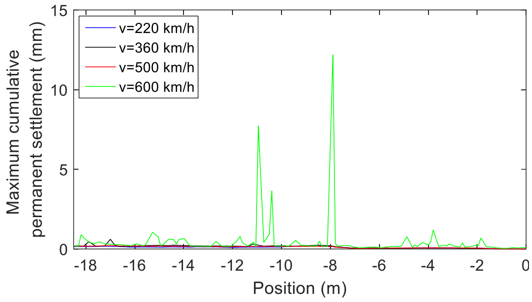

b) FPL with the train speed between 220 km/h and 600 km/h

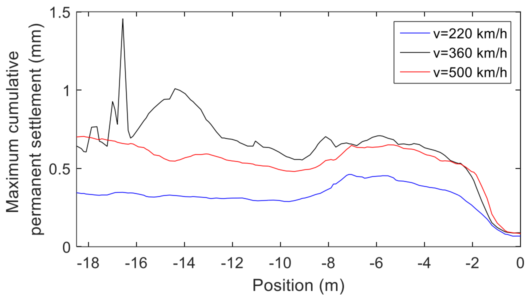

c) subgrade with the train speed between 220 km/h and 500 km

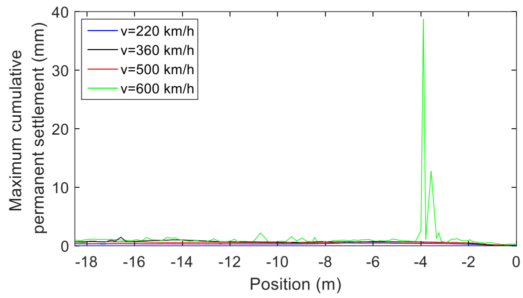

d) the subgrade with the train speed between 220 km/h and 600 km/h

Figure 4. Maximum cumulative permanent settlement

4 Conclusions and Contributions

This work presents an in-depth study on the performance of a ballastless track within transition zones, taking into account the influence of the train speed, including the critical speed. Thus, a novel hybrid approach to simulate track degradation was developed and applied based on a robust and advanced 3D Finite Element Model using ANSYS, enabling the assessment of the track's short-term performance. Soil settlement was simulated through the implementation of a calibrated empirical permanent deformation model.

Regarding the short-term performance, the displacements and accelerations induced in the track elements Both displacements and accelerations exhibited a direct increase with the augmentation of train speed. Notably, the magnitude of this increase was most pronounced when the train speed approached the critical speed (600 km/h).

The long-term results indicated that settlement in the substructure significantly increased when the train speed reached 600 km/h. In fact, the maximum cumulative permanent settlement exceeded the allowable limits at this speed. However, for other speeds, permanent deformation increased but did not exhibit a substantial magnitude difference.

Acknowledgements

This work was partially carried out under the framework of In2Track3, a research project of Shift2Rail. This work was also partly financed by FCT / MCTES through national funds (PIDDAC) under the R&D Unit Institute for Sustainability and Innovation in Structural Engineering (ISISE), under reference UIDB / 04029/2020. It has been also financially supported by: Base Funding – UIDB/04708/2020 of the CONSTRUCT – Institute of R&D in Structures and Construction – funded by national funds through the FCT/MCTES (PIDDAC).

References

[1] Indraratna, B., M. Babar Sajjad, T. Ngo, A. Gomes Correia, and R. Kelly, *Improved performance of ballasted tracks at transition zones: A review of experimental and modelling approaches.* Transportation Geotechnics, 2019. **21**.10.1016/j.trgeo.2019.100260

[2] Ramos, A., A. Gomes Correia, R. Calçada, and D.P. Connolly, *Ballastless railway track transition zones: An embankment to tunnel analysis.* Transportation Geotechnics, 2022. **33**: p. 100728.https://doi.org/10.1016/j.trgeo.2022.100728

[3] 3. Frohling, R.D., H. Scheffel, and W. EbersÖHn, *The Vertical Dynamic Response of a Rail Vehicle caused by Track Stiffness Variations along the Track.* Vehicle System Dynamics, 1996. **25**(sup1): p. 175-187.10.1080/00423119608969194

[4] Hunt, H.E.M., *Settlement of railway track near bridge abutments.* Proceedings of the Institution of Civil Engineers: Transport, 1997. **123**(1): p. 68-73.10.1680/itran.1997.29182

[5] Nicks, J., *The bump at the end of the railway bridge*. 2009, Texas A&M University

[6] Paixão, A., E. Fortunato, and R. Calçada, *A contribution for integrated analysis of railway track performance at transition zones and other discontinuities.* Construction and Building Materials, 2016. **111**: p. 699-709.https://doi.org/10.1016/j.conbuildmat.2016.02.126

[7] Banimahd, M., P.K. Woodward, J. Kennedy, and G.M. Medero, *Behaviour of train-track interaction in stiffness transitions.* Proceedings of the Institution of Civil Engineers: Transport, 2012. **165**(3): p. 205-214.10.1680/tran.10.00030

[8] Grossoni, I., S. Hawksbee, P. Jorge, Y. Bezin, and H. Magalhaes, *Prediction of track settlement at high-speed railway transitions between embankment and bridge in the proximity of a turnout.* Transportation Geotechnics, 2022. **37**: p. 100879.https://doi.org/10.1016/j.trgeo.2022.100879

[9] Matias, S.R. and P.A. Ferreira, *The role of railway traffic and extreme weather on slab track long-term performance.* Construction and Building Materials, 2022. **322**.10.1016/j.conbuildmat.2022.126445

[10] Gu, Q., C. Zhao, X. Bian, J.P. Morrissey, and J.Y. Ooi, *Trackbed settlement and associated ballast degradation due to repeated train moving loads.* Soil Dynamics and Earthquake Engineering, 2022. **153**: p. 107109.https://doi.org/10.1016/j.soildyn.2021.107109

[11] Ramos, A., A. Gomes Correia, R. Calçada, P. Alves Costa, A. Esen, P.K. Woodward, D.P. Connolly, and O. Laghrouche, *Influence of track foundation on the performance of ballast and concrete slab tracks under cyclic loading: Physical modelling and numerical model calibration.* Construction and Building Materials, 2021. **277**: p. 122245.https://doi.org/10.1016/j.conbuildmat.2021.122245
[12] Chen, R., J. Chen, X. Zhao, X. Bian, and Y. Chen, *Cumulative settlement of track subgrade in high-speed railway under varying water levels.* International Journal of Rail Transportation, 2014. **2**(4): p. 205–220.10.1080/23248378.2014.959083